Chapter 3

Speckle Correlation technique for measurement of optical properties

3.1 Introduction for Optical Rotation

Light has various aspects associated with it; one such property is Polarization. The utilization of polarization characteristics of light has increased significantly in recent years. A large amount of information can be obtained by detecting and quantifying the polarization states of light which can be applied in various fields including imaging [56] and biomedical diagnosis [57,58]. Optical Rotation measurement plays a crucial role in the measurement of the state of polarization and is widely applied in many critical fields including sugar manufacturing, chemical and pharmaceutical industries, environmental monitoring, and biomedical applications [59].

This chapter demonstrates the application of a laser speckle based optical technique that uses a speckle correlation algorithm to measure optical rotation. The phenomenon of polarization and optical birefringence serves as the basis for studying optical rotation. To pursue this study, quantification of optical rotation that is observed in the cases of Faraday rotation as well as optical activity is taken into consideration.

Polarization is a very crucial property that characterizes the Electromagnetic (EM) radiation according to the direction of the vibrating electric field. As the nature of EM waves is transverse in the far field regime, the direction of the oscillating field will always be perpendicular to the direction of propagation. If the direction and magnitude of the electric field randomly vary with time the EM radiation is said to be randomly polarized whereas if the direction of the electric field follows a specific pattern while propagation it is known as polarized light. And depending on the variation in the direction of the electric field vector, polarization of light can broadly be classified into three categories namely Linear Polarization, Elliptical Polarization and Circular Polarization [60].

It is observed that many crystalline substances are optically anisotropic in nature as there is a non-uniform spatial distribution of refractive index which leads to different values for speed of propagation being obtained whenever a specimen is inspected from different directions whereas the isotropic substances are symmetrical in nature and thus generate identical results for speed of propagation in all inspection directions. The properties of the material may vary depending upon the probing modalities such as optical, thermal, acoustical, magnetic, electric, etc. In anisotropic crystals, due to the presence of a crystallographically distinct axis, the interaction of light depends upon the orientation of the crystalline lattice with respect to the angle of the probe beam.

An optically anisotropic material can possess an orientation-dependent refractive index distribution that can lead to a condition known as birefringence which is also defined as the double refraction of light. Light entering the anisotropic crystal along the optical axis behaves similar to as it would have behaved while interacting with isotropic crystal and this passes through the crystal with a single velocity. However, when the light enters along a non-equivalent axis, it encounters two different refractive indices which make the light refract into two rays, each polarized along the two orthogonal directions and travel at different velocities. One of the rays obeys the laws of normal refraction and travels with the same velocity in every direction through the crystal which is termed as ordinary ray, while the other ray travels with a velocity that is dependent upon the propagation direction within the crystal and is termed as the extraordinary ray. Therefore, each polarized light ray entering the crystal is split into an ordinary and an extraordinary ray that emerges from the distant end of the crystal as linearly, circularly and elliptically polarized rays depending upon the distance of propagation inside the crystal.

Since the visible light consists of electric and magnetic components, it’s velocity through the substance also depends upon the electrical conductivity of the material. Thus, the dielectric constant of the material plays a very crucial role in defining the speed of electrical signals traveling through the medium. How a light wave interacts

with the crystal through which it passes depends on the inherent orientation of the lattice's electrical vectors and the direction of the wave's electric vector component.

Optical birefringence can be observed in optically anisotropic materials. Some materials show birefringence when subjected to an external force (ex. a magnetic field) while some materials produce birefringence owing to their specific structural properties. Optical rotation caused by these two phenomena is quantified by measuring optical rotation caused by Faraday Effect and Optical Activity separately [61].

3.1.1 Faraday Effect

One of the ways with which the light interacts with matter is by interacting with the magnetic state of the medium wherein the electronic structure and motion of the matter are involved. The Magneto-optic effects are observed when such interaction between EM radiation and magnetically polarized materials takes place. Similar effects can be observed in the case where certain specific materials under the effect of the electric field modulate some properties of light passing through it [60,62]. The phenomenon of birefringence observed in some optical medium while it is subjected to either magnetic field or electric field can be explained by understanding the magneto-optic and electro-optic effects. The Magneto-optic effects comprise the Larmor precession [63,64], Zeeman effect [65] and Faraday effect [66] while the electro-optic includes the Stark effect [67], Pockels effect [68] and Kerr effect [69].

The Larmor precession is the precession of the magnetic moments of charged particles in the external magnetic field whereas the Zeeman effect is the splitting of a spectral line into several components in the presence of a static magnetic field. The Faraday rotation accounts for the interaction between medium subjected to a magnetic field where the linearly polarized light rotates upon passing through the optical medium. An electric analog of the Zeeman effect is the Stark effect where shifting and splitting of spectral lines of the charged particles take place in the external static electric field. In the case of the Pockels effect, the birefringence is

directly proportional to the electric field whereas in the case of the Kerr effect it is proportional to the square of the electric field [63–69].

3.1.1.1 Theory for Faraday Rotation

This chapter deals with the Faraday Effect which was discovered in 1845 by Michael Faraday. He noticed that the plane of polarization of a linearly polarized light was rotated upon propagating through an optical medium which was subjected to a magnetic field parallel to the propagation direction. These were some of the few initial observations that indicated the interaction between the magnetic field and the light. The Faraday effect along with the magneto-optical Kerr effect are widely used for the detection of magnetization in materials [70–74].

Faraday Effect is caused due to circular birefringence, making the two oppositely headed (left and right) waves to propagate at different velocities [60]. This effect is used in several applications such as analysis of a mixture of hydrocarbons, modulators, etc. [74] and it has applicability in optics [75–77] and plasma diagnostics [78].

There are various ways to measure the faraday rotation using optical means [79–87] based on the change in the polarization rotation angle of light beam propagating through magneto-optic materials. This angle of rotation of plane of polarization of liner polarized light is given by

$$\theta = \vartheta BL = \pi L \Delta n(B) \Big/ \lambda_0 \tag{3.1}$$

where ϑ is Verdet constant, B is the applied magnetic field and L is the interaction length (length of the magneto-optic medium). λ_0 is the wavelength of light in vacuum and Δn is the difference in the index of refraction between two circularly polarization states leading to the rotation. Conventionally, a positive Verdet constant corresponds to a (diamagnetic) material for which the Faraday Effect is *l-rotatory* (anticlockwise rotation) when the light moves parallel to the applied magnetic field and *d-rotatory* (clockwise rotation) when it propagates antiparallel to the applied magnetic field [5]. Most materials showing the Faraday

Effect have small Verdet coefficients. For example, the Verdet constant at 611.8 nm for Quartz is only 0.01543 arcmin/G cm [88]. This will lead to small rotations of linearly polarized light for low magnetic fields (less than 1° at the magnetic field of 200 G for a sample of 15 cm length). This is true for most of the materials showing the Faraday Effect [74]. So by using Malus's law, cross polarizer pair [74] and conventional detectors like photodiodes it may be difficult to accurately measure these small rotations, which are of high interest. Methods with higher sensitivity need to be developed for these measurements.

When a laser beam with sufficient coherence length illuminates a rough surface, it generates a random interference pattern called the speckle field (volume phenomenon). These speckles can be captured directly by a photosensor such as a CCD chip, leading to an objective speckle pattern. The shape and size of these depends on the surface which produces it as well as on the properties of the incident wavefront. Any change in the properties of the incident wavefront will lead to changes in the speckle pattern [89]. So, a change in the polarization state of the incident wavefront produces a change in the detected speckle field. This effect can be used to determine the change in the angle of rotation of polarization. Here a method that uses objective speckle patterns generated by a ground glass diffuser, to determine very small changes in the rotation of the plane of polarization produced by magneto-optic materials is presented [90].

3.1.1.2 Experimental setup for Faraday Rotation Measurement

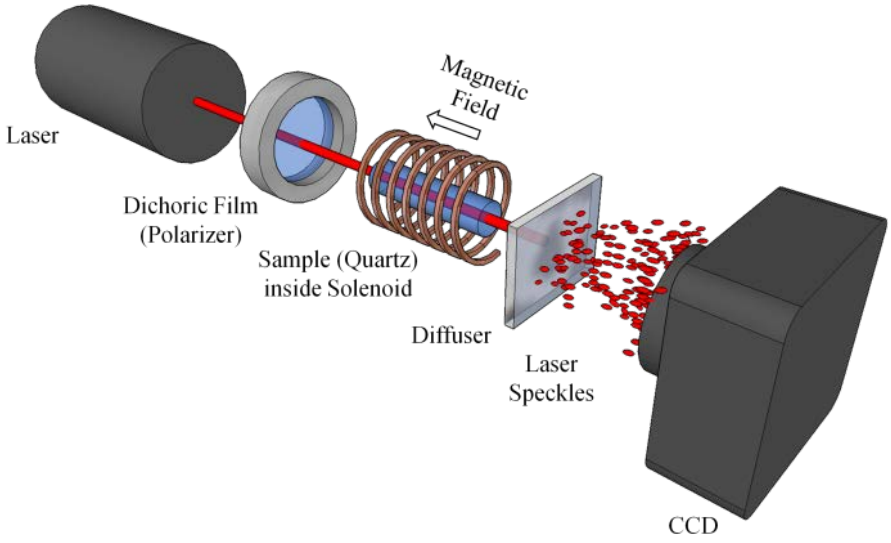

Fig 3. 1: Speckle-based sensor for low field Faraday rotation measurement

Fig. 3.1 shows the experimental setup. In the present study, a He-Ne laser (unpolarized, 611.8 nm, maximum output power <2 mW) is used as the light source. Any laser (including a diode laser) with sufficient coherence length can be used as the source. The beam is linearly polarized using a dichroic film and then passed through the sample (quartz crystal) under investigation, which is kept along the axis of a solenoid (having 175 turns/cm) used to apply an axial magnetic field. On the exit side of the medium, a ground glass diffuser is placed to convert the laser beam into a volume speckle field. The objective speckle field is sampled using a CCD camera (AVT Guppy-146 C, 8-bit dynamic range, 4.65 μm pixel pitch, 512 × 512 pixels exposed) connected to a PC.

An unexpanded laser beam (diameter ~ 1 mm) without spatial filtering is used and the CCD is placed 7 cm away from the diffuser so that the sampling criteria, i.e. speckle size ($\rho_o \approx \lambda d / D$) is twice the detector pixel size-is satisfied. Magnetic fields of different strengths are applied along the axial direction by passing different amounts of electrical current through the solenoid coil. This magnetic field rotates the plane of polarization of the incident linearly polarized light according to Eq. (3.1). The diffuser, which has a rough surface with random surface variations,

creates spatially changing random angles of incidences for the laser beam, which can be treated as a plane wave. The transmittance and reflectance of any dielectric depends upon the angle of incidence are given by the Fresnel's equation [60]. Since the transmittance and the reflectance of the incident beam depends upon the angle of incidence, which in turn depends upon the state of polarization, the complex amplitude of the laser beam at the output face of the diffuser changes with polarization thereby changing the resulting speckle field [91]. The correlation coefficient of the sampled speckle patterns intensities [89] with and without the applied magnetic field can then be used as a measurement of the rotation. For each applied magnetic field, objective speckles patterns are recorded for 30 s at the rate of 1 Hz and stored for analysis.

3.1.1.3 Calibration and Measurements

The setup is calibrated using a 15 cm fused quartz rod and having a Verdet constant of 0.01543 arcmin/G cm (at 25 °C) for 611.8 nm. Calibration is carried out using two sets of magnetic fields: (i) ranging from 0 G to 206 G at 15 G interval and (ii) 0 to 26 G at 1.5 G interval. The two calibrations are done to check whether the variation is the same (linear) in both ranges so that it can be established that a single calibration curve can be used to measure unknown rotations of the polarization state. First, a series of reference speckle patterns are recorded for 30 s at 1 Hz. For the reference set, no magnetic field is applied and hence there should not be any rotation. When the magnetic field is applied, the plane of polarization of the beam rotates [74]. Correlation coefficients and the change in correlation coefficient are determined with all the 512 × 512 pixels using Eq. (2.8) and Eq. (2.9) respectively. The time variation in the speckle decorrelation for the speckle pattern recorded without applying any magnetic field determines the minimum measurable optical rotation. The reason for the time variation in the speckle decorrelation can be attributed to mechanical vibrations of the system and fluctuations in the source as well the recording device.

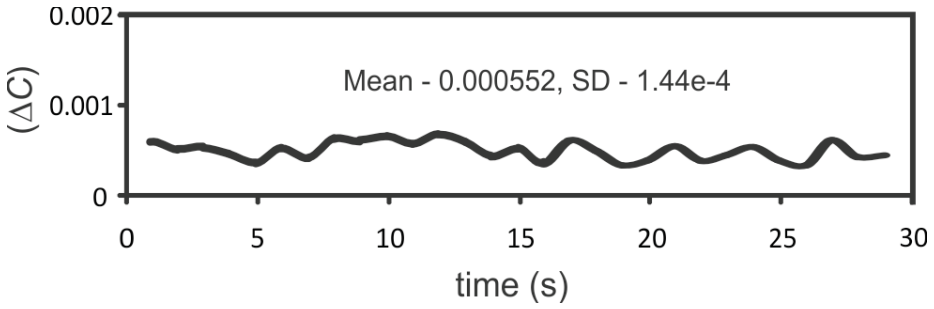

Fig 3. 2: Change in the speckle correlation coefficient as a function of time for reference speckle pattern (no applied field). Standard deviation determines the minimum measurable rotation, which in this case is 0.0025°.

Fig. 3.2 shows the change in the correlation coefficient (ΔC) for the series of reference patterns when compared to the first speckle pattern in the series. The standard deviation of this series determines the minimum measurable rotation. For each applied field, 30 speckle patterns were sampled at 1 Hz. For each of these speckle patterns, the correlation coefficient with every one of the reference frames is computed and time-averaged. The measurement system is calibrated from these time-averaged values.

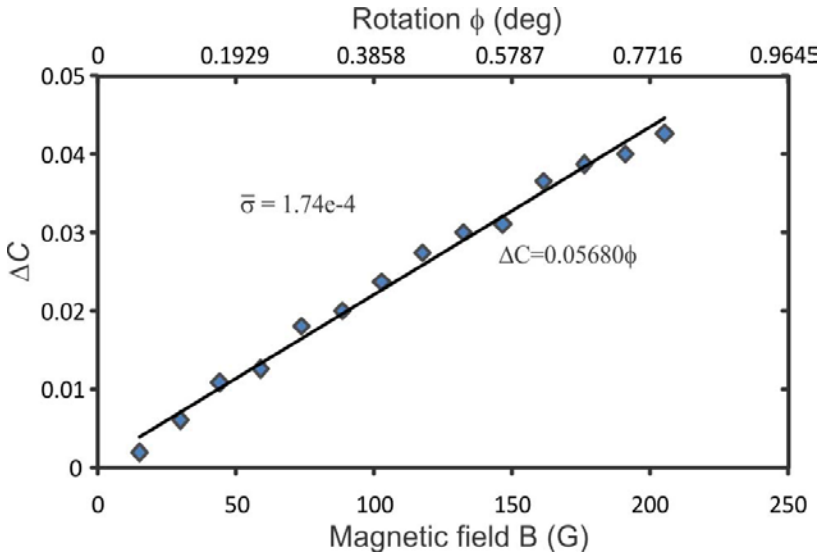

Fig 3. 3: Change in the speckle correlation coefficient (ΔC) versus the change in the strength of the applied magnetic field. Axis on top gives the corresponding rotation of the plane-polarized light. The straight line represents the linear fit to the measured values.

Fig. 3.3 shows the obtained calibration plot for the magnetic fields from 0 to 205 G (the magnetic field was varied by 15 G). The measurements are repeated with applied fields ranging from 0 to 26 G. Fig. 3.4 shows the computed change in the speckle correlation coefficient as a function of the applied field for this range. From Fig. 3.3 and Fig 3.4 it can be seen that the variation in the speckle correlation coefficient (ΔC)with the applied field is linear, as expected from Eq. (3.1), even for very small applied magnetic fields, which leads to small optical rotations. Both curves (for large and small field variations) have almost the same linear dependence on the field/rotation. These calibration plots are then used for the measurement of unknown rotations. To compare the advantage of the proposed technique with the polarization rotation measurement using polarizer analyzer pair, the experiments are repeated by replacing the diffuser with an analyzer (a second polarizer rotated 90° to the first one). The output from the analyzer is measured using a silicon photodiode (responsivity of 0.38 A/W at 600 nm) coupled to an amplifier with a voltage gain of 500 and a digital meter. Detector outputs for different applied magnetic fields are measured several times and averaged.

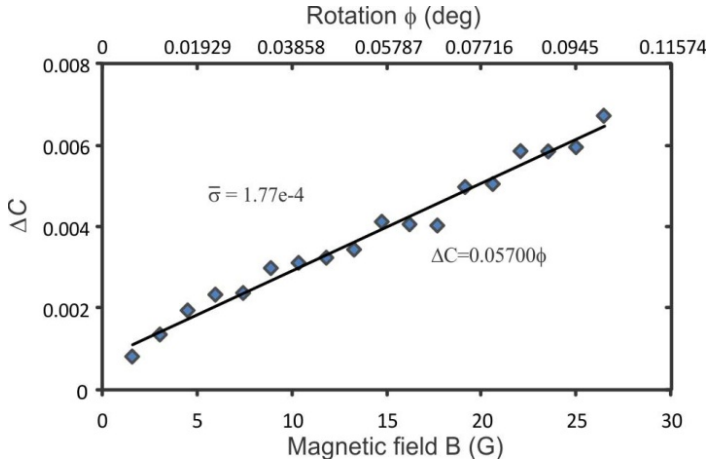

Fig 3. 4: Change in the speckle correlation coefficient (ΔC) for magnetic field variation from 0 to 26 G.

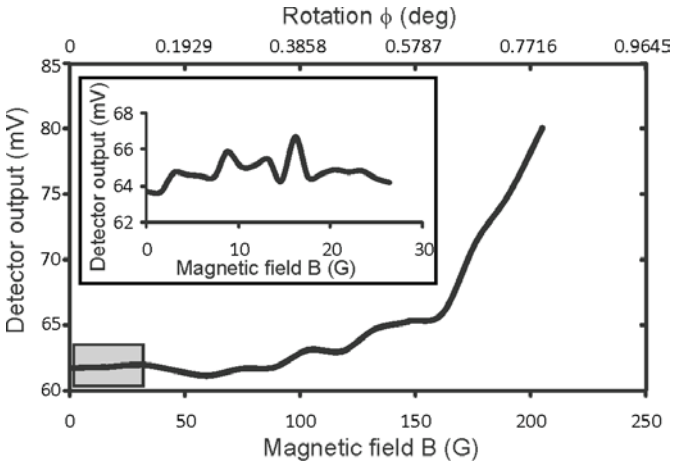

Fig 3. 5: Rotation measurement with crossed polarizer-analyzer pair. The main figure shows the photodiode output as a function of the applied magnetic field. The inset shows the variation in the detector output in the shaded portion (low magnetic fields).

Fig. 3.5 shows the measured variation in detector output with the applied field. Comparing Fig. 3.5 to Fig. 3.3 and Fig. 3.4, it can be seen that the measurement system using the polarization analyzer pair is not sensitive enough to measure small optical rotations. Since the change in speckle intensity distribution is much higher even for small change in state of polarization compared to the to the approach based on Malus's law, the speckle correlation based approach will be much more sensitive. Note that the rotation of polarization is related to the relative change in the refractive index (sensed by one polarization state with respect to the other). Change in the refractive index is equivalent to the change in the optical path. As the propagation of the optical field may be approximated by the Fresnel integral, the change in the optical path yields an additional spatial quadratic phase inside the Fresnel integral. This quadratic phase changes the resulting speckle distribution and thus de-correlates the speckle distribution with respect to the distribution obtained without applying the magnetic field (i.e. without modifying the optical path). The minimum magnetic field producing the de-correlation process for a given propagation distance L inside the medium can be estimated by using Eq. (3.1) which provides the change in the optical path (which is connected to the change in the refractive index and the polarization rotation) and by connecting it to the quadratic phase appearing in the Fresnel integral.

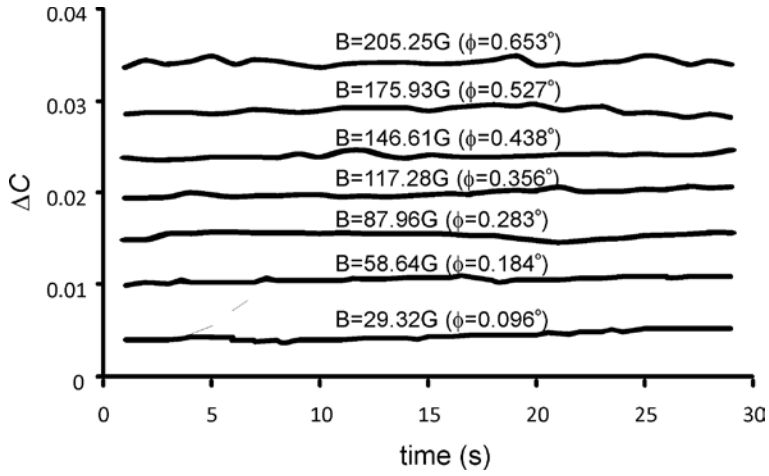

Fig 3. 6: Change in the speckle correlation coefficient (ΔC) with time for different strengths of the applied magnetic field for a quartz rod with a 12-cm length. Note that the lines are equally spaced, which indicates a linear relationship between the variation in rotation and the strength of the magnetic field

Fused Quartz rods of varying lengths are used as objects for measurement purposes. They are kept along the axis of the solenoid described in the setup and varying magnetic fields were applied by changing the current. For all the objects used in measurement, 30 speckles patterns are recorded for each applied field. Also, 30 reference frames (without applied field but with the sample present) are recorded for each sample. Using a separate reference for each sample reduces the error which might be introduced either due to the sample properties or due to physical disturbance in the system. For each time instance, the correlation coefficient of the object frame with each reference frame is computed and was averaged. Fig. 3.6 shows the variation with time of the correlation coefficient when a 12 cm long Quartz rod was used as the sample for various applied field strengths. It can be seen that the variation is constant in time and the lines are equally spaced, indicating a linear change in rotation of polarization with the applied field.

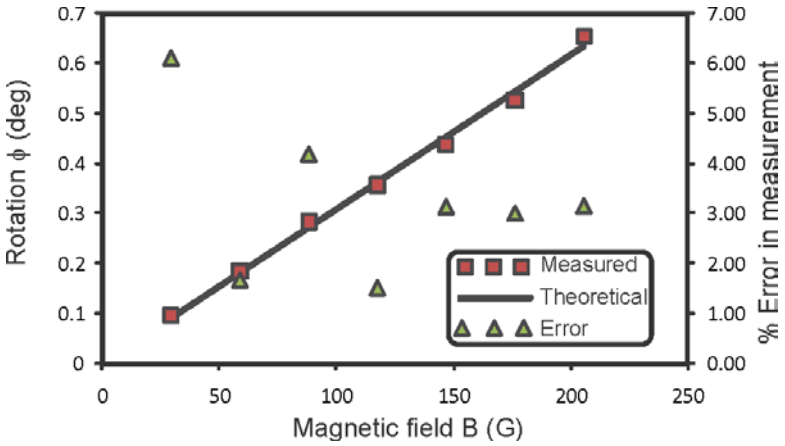

Fig 3. 7: Measured Faraday rotation using change in the speckle correlation coefficient (for a rod of 12 cm length). Straight-line indicates values calculated theoretically. Triangles represent the error in measurement.

Fig. 3.7 shows the measured rotation using the calibration plot in Fig. 3.3 along with the theoretically calculated values. The figure also shows the error in measurement for a 12 cm quartz rod. The error is calculated by comparing the measured values with theoretical values. The measurement shows a linear variation with the applied magnetic field. The measured values are equally spaced mirroring the linear variation in the magnetic field. Here rotation change of 0.0917 degrees could be measured with a 3.3% error. In the next set of measurements, a 10 cm Quartz rod is used as the sample and the field was varied from 0 to 26 G to check the measurement accuracy at very low rotation angles.

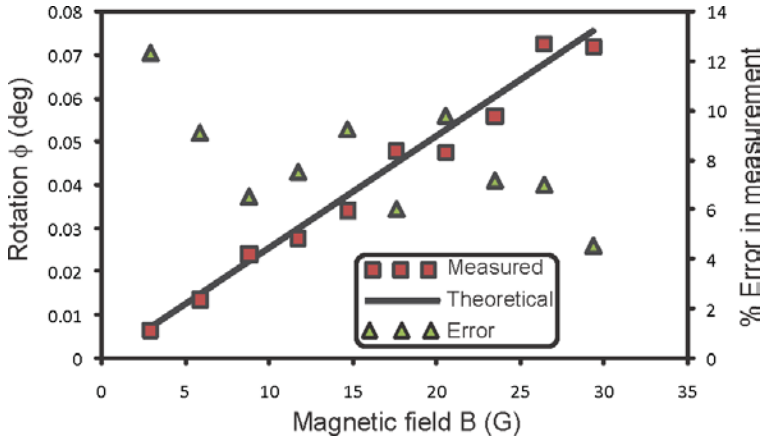

Fig 3. 8: Measured Faraday rotations for small changes in the magnetic field (rod of 10-cm length). Note that the error in measurement has increased compared to Fig. 3.7

Fig. 3.8 shows the measured (using the calibration plot in Fig. 4) as well as theoretically computed values for this case. The measured rotation change is 0.0066 degrees with 92% accuracy. The proposed technique is also tested by coupling it to a cell phone camera to demonstrate that the technique can be made into a field-portable handheld device.

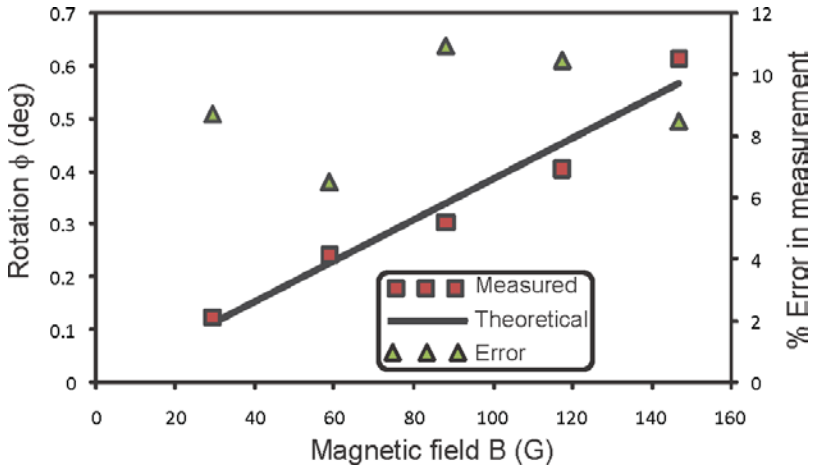

Fig 3. 9: Measured rotation using change in the speckle correlation coefficient for a quartz rod with a length of 15 cm using a cell phone camera as the speckle field detector

Fig. 3.9 depicts the measured rotation using a cell phone camera (LG KP500) instead of the CCD sensor (after calibration). For each applied field 30-second videos (QVGA at 12 fps) are recorded and the frames then extracted to compute the speckle correlation coefficient values with reference frames. Higher dynamic range of the sensor can provide better decorrelation values thereby increasing the sensitivity of the system. In summary, we have demonstrated the development of a speckle-based sensor for measurements of small rotations of the plane of polarization of linearly polarized light and applied it for measurement of small field Faraday rotations. The method could also be used to sense magnetic fields. But magnetic field sensors today are very sensitive and can sense even fields of 0.1 nT, i.e. 6 orders of magnitude less than 1 G (what we have measured). However, the rotation angle is a product between the field and the Verdet constant. In our experiments, we used Quartz having relatively small Verdet constant. Also, the distance propagated through the medium is short. If for instance, we used material with higher Verdet constant or if we take a fiber of say 1 km long and packaged it,

it would be able to measure much smaller magnetic fields (e.g. as small as few tens of pico Tesla). The proposed technique may be a useful measurement tool especially when the state of polarization can be used to quantify physical parameters. One of the applications is in the area of sugar level measurement in fluids. Sugar is optically active and it rotates the linearly polarized light. The method could measure the level of sugar by measuring the rotation and then converting it to the concentration of the sugar in the fluid.

3.1.2 Optical Activity

The phenomenon of optical activity is observed in a large number of organic compounds and many complex compounds of metals (like transition Ni, Co), the organometallic compounds, as well as liquid crystals [92]. Moreover, in the domain of biomedical sciences, proteins, DNA and RNA, chlorophyll, hemoglobin, etc. have shown some signs of optical activity [93,94]. Most of the amino acids which are considered to be the building blocks of life are optically active and hence the methods of measuring optical activity are employed to investigate samples from extraterrestrial sources to predict the existence of life on other planets [95,96].

Optical activity brings about a change in the state of the polarization of the linearly polarized light and its measurement can provide very significant information about the molecular structure and the concentration of a chemical [97], especially blood glucose concentration [98–100]. Blood glucose monitoring is required in body fluids to maintain the glucose level in diabetes mellitus in which dietary regulations are required [101–105]. Sugar being optically active material, measurement of sugar concentration is also required in areas like food industries where the sugar levels in juices, other beverages, and food items have to be maintained. This is required for proper taste as well as to sense adulteration in juices [106]. In the area of agricultural sciences, sugar level measurement becomes necessary to test the quality of crops, vegetables, and fruits [107]. Therefore, the task of studying the optical activity of substance plays a huge role in biophysics, biochemistry, medicine, agriculture, and pharmaceutical industries.

3.1.2.1 Theory of Optical Activity

The phenomenon of optical activity was first observed in 1811 by the French physicist F.J. Arago and during the same era, Jean Baptiste Biot saw this same effect using both the vaporous and liquid forms of various natural substances like turpentine [60]. The optical activity demonstrated by various materials is associated with the chiroptical (Chiral-optical) effects which were discovered in 1848 by Pasteur [108], who investigated two types of tartaric acid crystals and described the structure of the crystals as if "they look at each other in the mirror" [109]. Chiral molecules are pairs of molecules in which one is the non-superimposable mirror image of the other. Chiral molecules are also known as enantiomers or optical isomers. Chiral molecules have identical physical and chemical characteristics except for the way with which they interact with polarized light. One of the enantiomers rotates the electric field vector of polarized light in the clockwise direction while the other rotates it in the counterclockwise direction by the same degree. Moreover, many biological stereospecific molecules interact differently with the enantiomers and thus it becomes very crucial in the pharmaceutical industry as one enantiomer of a drug may have the intended medicinal effect while the other can be ineffective or even highly toxic [110].

Optically active materials rotate the plane of polarization of incident linearly polarized light. It also becomes very essential to distinguish between right and left-handed rotation. While looking in the direction of the source, if the plane-of-vibration appears to have revolved clockwise then the material is referred to as *dextrorotatory* of *d-rotatory* and if it revolves anti-clockwise the material is referred to as *levorotatory* or *l-rotatory*[60]. To understand the concept governing the rotation, a linearly polarized wave is considered which can be represented as the superposition of right circularly (R) and Left circularly (L) polarized states. Sugar shows optical activity in which R and L states propagate at different velocities in sugar solution. In an optically active medium, R and L states encounter different refractive indices and hence propagate with different velocities leading to a phase difference between the two components at the exit face of the material medium. At the exit face, the two circular polarization states will combine again to form linearly

polarized light. The phase difference between the two circular waves while passing through the optically active sample leads to the rotation of linearly polarized waves with respect to the incident linearly polarized state. The angle of rotation of the plane-of-polarization is proportional to both the concentration of the active material in the solution as well as the length of propagation and is given[60]

$$\beta = \frac{2\pi}{\lambda_0}(n_L - n_R)d = sdc \tag{3.3}$$

where λ_0 is the vacuum wavelength of the light source, n_L and n_R are the refractive indices of left and right circularly polarized light, d is the length of the sample, s is the specific rotation (rotation/unit length/unit concentration) of the sample and *c* is the concentration of the sample. The rotatory power of the medium is β/d and from Eq. (3.3) it can be seen that the rotatory power varies with concentration [60].

It is very essential to differentiate between the rotation associated with the Faraday rotation and the Optical Activity. The direction of rotation is reversed in case of Faraday Effect when the direction of propagation of linearly polarized light with respect to the direction of the applied magnetic field is reversed whereas in the case of optical activity the direction of rotation is the same even if the direction of propagation of the light is reversed. For example, consider a magnetic field generated by a solenoidal coil wound about the sample. The plane of vibration, when the Verdet constant is positive, rotates in the same direction as the current regardless of the beam's propagation direction along its axis [60].

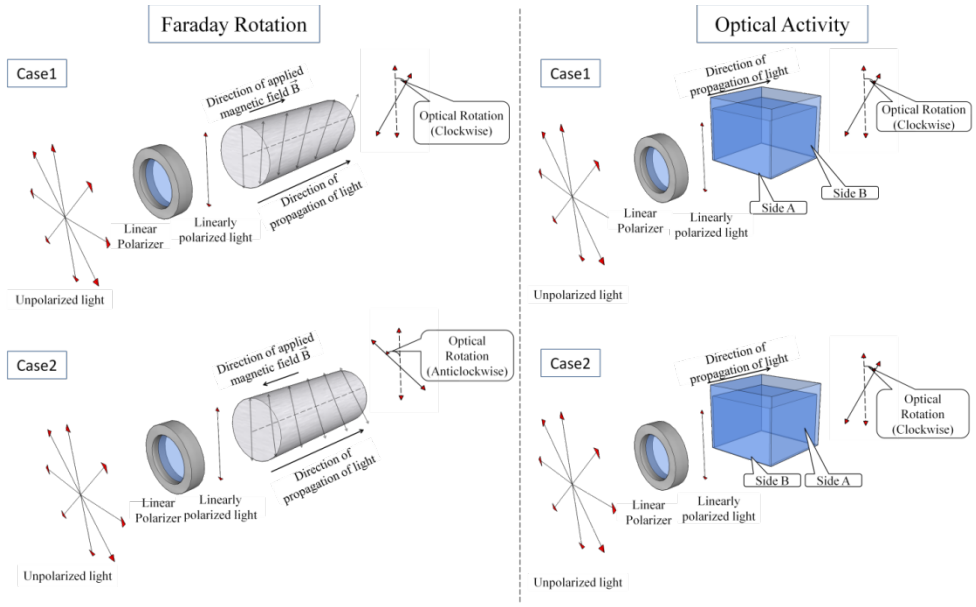

Fig 3. 10: Faraday Rotation Case1: Applied Magnetic field parallel to the direction of propagation of light. Case2: Applied Magnetic Field antiparallel to the direction of propagation of light. Optical Activity Case1: light entering the chamber containing optical active material from Side A and leaving from Side B. Case2: The light entering the chamber from Side B and leaving from Side A

Fig. 3.10 describes the differences between the optical rotation due to the Faraday Effect and the optical activity. It can be seen in the case of Faraday Rotation that by changing the direction of the magnetic field the direction of the rotation is reversed. On the other hand, in the case of the optical activity by reversing the direction of propagation of light through the chamber containing the optically active solution, the direction of rotation remains unchanged.

Many researchers have worked towards exploring optical activity due to which various techniques have been developed over the years for measuring optically activity. Thus detecting and quantifying optical activity, glucose level could be measured etc[49,111–119]. In the case of glucose sensing in the human body, both continuous and point sampling can be used [120]. The point sample techniques involve invasive techniques such as drawing body fluids by finger pricking, which can be painful and have some disadvantages like damaging the tissues and is not practical for continuous monitoring [104,121]. While in the case of continuous sampling techniques, both invasive and non-invasive techniques can be employed.

Most of the non-invasive techniques in continuous sampling methods are optical [104,121,122] since optical techniques are easy to implement and in many cases do not use any chemical reagents and are also fast [104]. Optical techniques for sugar level measurement includes Kromoscopy, Photoacoustic spectroscopy, Optical coherence tomography, Scattering/occlusion spectroscopy, Polarimetry, Thermal infrared, Fluorescence, Raman spectroscopy, MIR spectroscopy, NIR spectroscopy, etc [120]. Speckle based non-invasive techniques are also reported for non-invasive measurement of glucose concentration in blood. These techniques are based on different principles of measurement having characteristic advantages and disadvantages [54,121]. Sugar level monitors used in food and agricultural products include electronic tongues, Spectroscopic and chromatographic techniques. These techniques analyze the chemical composition to measure the sugar concentration in the food and agricultural products [106]. Refractometric, hydrometric and densitometry techniques are also used for sugar content measurement to test the crop quality [123].

Polarimetry uses the optical rotatory power of sugar to measure its concentration. Rotation of plane of polarization of linearly polarized light is proportional to the concentration of sugar in the solution. This technique can be used to measure the concentration of glucose by passing light through a sample, especially through aqueous humor of eye where glucose is most likely to be present [101,120,124]. But using a polarizer analyzer pair, commercially available detectors, and Malus law it becomes difficult to determine the change in the state of polarization when the concentration of an optically active medium under investigation is small. This makes the development of highly sensitive polarimetric methods necessary.

When the laser beam falls on a rough surface like that of a ground glass diffuser, due to the random surface variations of the diffuser, the laser beam exhibit spatially varying random angles of incidence. As the transmittance, as well as the reflectance of the incident beam, depends upon the angle of incidence, the complex amplitude of the laser beam at the output face of the diffuser changes with the changing polarization states which in turn is caused by the optical activity of sugar solution

and thereby changing the resulting speckle field [52,53,91]. So, the speckle field at different concentrations of sugar solutions will have different shapes and sizes. By comparing the obtained speckle field for a particular known sugar concentration with a reference speckle field, the technique can be calibrated.

It has already been discussed that the proposed speckle correlation technique is used for the measurement of small rotations of linearly polarized light in the case of magneto-optic materials [52].Here we present a simple, compact, cost-effective way to measure sugar concentration using a speckle de-correlation technique.

3.1.2.2 Experimental Setup for measurement of Optical Rotation due to Optical Activity

Fig. 3.11 shows the schematic of the proposed technique. It comprises of a laser diode module working at 635nm with a maximum output power of 4.5mW. This laser beam is linearly polarized and then is allowed to pass through the experimental cell of length 1cm. The beam after passing through the solution under investigation falls on a ground glass diffuser. The diffuser is used to convert the laser beam into a volume speckle pattern. The aperture size of the diffuser is limited to 1mm in diameter using a diaphragm. The speckle pattern generated by the diffuser is then sampled using a CMOS sensor having a 1.67μm pixel pitch. The sensor is placed 4cm behind the diffuser to satisfy the sampling criteria (speckle size is at least twice the detector pixel size).

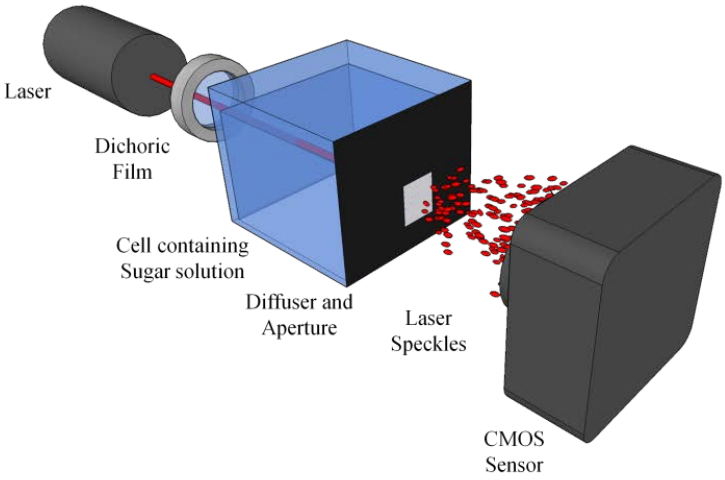

Fig 3. 11: Experimental setup for the measurement of sugar concentrations. Solutions having different sugar concentrations were obtained by dissolving different masses of sugar in distilled water

For each sugar concentration (sugar dissolved in distilled water) speckle patterns are recorded for 2s at the rate of 30Hz (total of 60 frames). Also, a reference speckle pattern with only distilled water in the experimental is recorded for the same duration. Fig. 3.12 shows the sample of the recorded speckle pattern for different sugar concentrations.

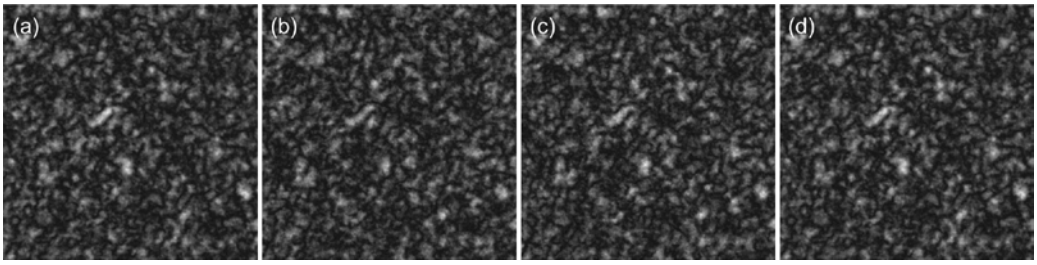

Fig 3. 12: Recorded speckle patterns for different sugar concentrations. (a) 0g/ml (distilled water only), (b) 0.01g/ml, (c) 0.05g/ml and (d) 0.1g/ml. For each concentration 60 patterns at 30Hz were recorded for comparison with the reference pattern (pattern recorded with distilled water)

Change in the speckle patterns due to concentration change is computed by comparing the speckle patterns recorded for solutions of different sugar concentrations inside the experimental cell with that recorded with distilled water inside the experimental cell. This correlation coefficient is calculated using Eq.

(2.8). This is repeated for all the recorded speckle patterns (at different time instances) for each concentration and the mean of the computed correlation coefficient at different time instances is determined. The change in correlation coefficient is computed from the obtained correlation value using Eq. (2.9).

The computed correlation coefficients with known concentrations are then used to find unknown concentrations from the calibration plot. It should be noted here that the standard deviation of the correlation coefficient for a particular sugar concentration obtained from the recorded speckle patterns by comparing the speckle patterns in different time instances determines the resolution of the system.

3.1.2.3 Calibration and Measurement

Experiments are conducted using sugar solutions of known concentrations to calibrate the setup. As mentioned in the previous section, speckle patterns after introducing the sugar solution in the experimental cells were recorded and using Eq. (2.8) and Eq. (2.9) the change in correlation coefficients was computed. For calibration, sugar concentrations varying from 0.01g/ml to 0.1g/ml with a step of 0.01g/ml are used. Also, for each concentration, ten data sets are recorded. The precision of the technique is the standard deviation of the correlation coefficient for the ten data sets. Fig. 3.13 shows the calibration curve of the technique.

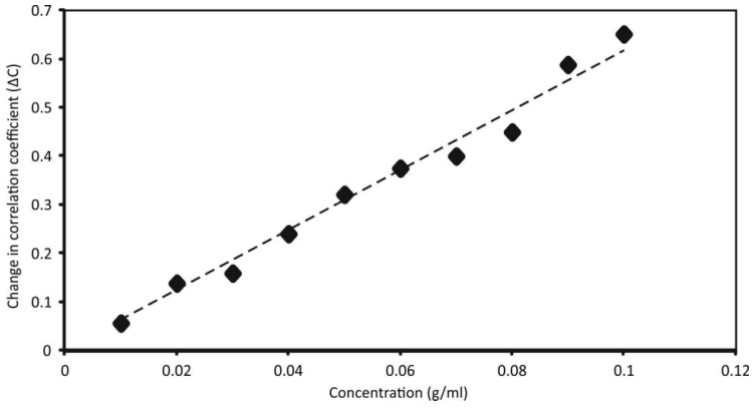

Fig 3. 13: Change in the correlation coefficient (ΔC) as a function of known sugar concentration. For each concentration, ten data sets were recorded. In the figure ♦ ♦ ♦ represent the mean of the DC obtained from all the data sets and - - - - - represents the linear fit to the experimental data

The resolution of the system is defined by the standard deviation of correlation coefficients obtained when the first speckle pattern is taken as reference and the rest of the frames are used as object frames of the same solution. The average resolution of the system by considering the obtained correlation coefficients for all the different sugar concentrations comes out to be 0.0030g/ml. The sensitivity of the system is obtained by taking the difference between the consecutive values of the correlation coefficient and taking an average of it over the concentration difference (0.01g/ml). The sensitivity turns out to be 6.432963 ΔC / (g/ml)`. The precision of the system is the standard deviation of the correlation coefficients obtained over all the concentration values and all the data sets and is 0.0011g/ml. To test the measurement ability of the system five known but different sugar solutions than those used for calibration were and the correlation coefficient change is measured experimentally. These Δ*C* values are used along with the calibration plot shown in Fig. 3.12 to determine sugar concentration. Fig. 3.14 shows the measurement results, from which it can be seen that the error in measurement is about 2.6%

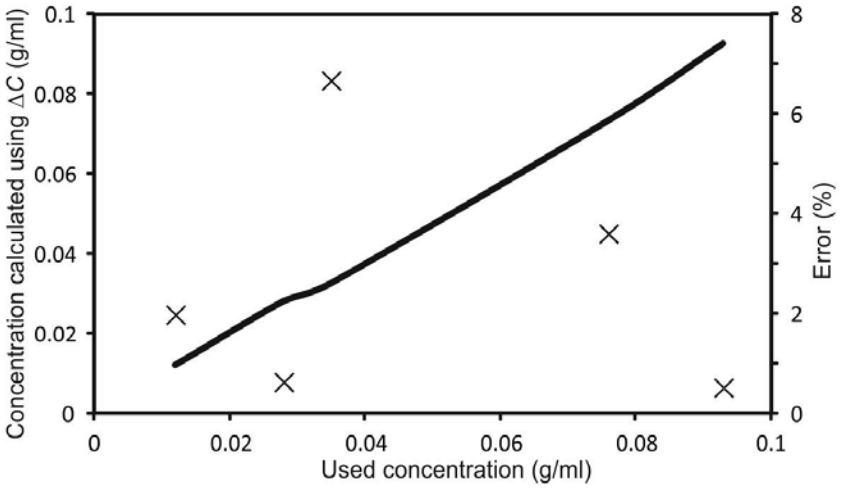

Fig 3. 14: Results obtained using unknown concentrations and the calibration curve

3.2 Refractive Index measurement

The manner in which electromagnetic radiation interacts with the medium generally provides an insight into the material's optical properties. As the electromagnetic

wave encounters the medium it interacts with the electrons of the medium and the electric field associated with the wave tends to vibrate these electrons. Due to these forced oscillations that are induced in the electrons, they reemit the radiation in terms of secondary sources of radiation thereby allowing EM wave to propagate in the material. Nevertheless, these secondary waves travel with a different speed (Normally lesser than the speed of light in vacuum) depending on the optical property of the material. This optical property, broadly speaking is a measure of material's ability to slow down the EM waves which is known as the Refractive Index [125–127].

Refractive index (RI) can be considered as one of the most important optical features of a material as one can find its application in all the major disciplines such as physics, chemistry, and biology [128]. Some of the specific areas where it is essential to measure refractive index accurately are communication systems, fiber optics, thick and thin films, polymers, in the pharmaceutical industry, food processing, and beverage industries [129–138]. In case of materials such as fused silica (glasses) and solid plastic, an account of the refractive indices can provide a measure about their transparency or clarity, while in case of fluids, the refractive index can be considered as a measure of dissolved substances or suspended microparticles [139]. Furthermore, knowledge of the refractive index can be very handy while interpreting various types of spectroscopic data. Analysis of the refractive index can also be very useful in scrutinizing the material or solution by dealing with the problem of adulteration. Thus, a quick, accurate and portable device to measure refractive index can be readily embraced [140]. Apart from the industrial applications, measurement of refractive index finds its utility in the field of biology as it is not only involved in the scattering of the light but also participates in the light-induced surface force on the biological object (example: a cell in the laser tweezer). To study the interaction of light with biological objects and its transportation in tissues, it becomes essential to acquire data regarding refractive indices of tissues as well as other biological specimens [134,141–145].

A whole range of methods and techniques for determining refractive index have been developed by employing various principles of physics and engineering. A very common and conventional method to determine the refractive index is to compute the angle of minimum deviation produced by a light beam while passing through the liquid contained in a hollow prism made of glass [60,128,146–148]. The refractive index can also be determined by measuring the deviation from the reference position of a light beam passing through the sample. The refractive index of water which is considered as the universal solvent has also been studied by many researchers by employing interferometric techniques like holography [149–153].

Another class of refractometers depends upon the use of optical fibers and are mostly based on total internal reflection (TIR) [154,155], evanescent waves [156], fiber Bragg grating (FBG) [157], surface plasmon resonance (SPR) effect [158–160], photonic crystal [161–163] etc. However, the refractometers based on the SPR effect, photonic crystals and FBG are very sensitive and they suffer from a common disadvantage of having a complex design. Moreover, these refractometers require expensive components for sensor design and characterization [129].

Ultrahigh sensitivity, compact size, and simple design can be offered by multimode interferometers (MMIs) [164–169] based on single-mode- no-core-single-mode (SNS). It is reported that SNS structure adopts wavelength modulation where RI is measured by monitoring the wavelength shifts of the selected dip or peak in the interference spectrum [168,170]. But these measurement techniques are costly and complicated as an optical spectrum analyzer (OSA) is used to detect the wavelength shifts [131].

Apart from direct measurement, information regarding the refractive index can be derived from physical properties such as the concentration of a transparent liquid. The relation between concentration and refractive index of the liquid has been explored by many researchers [170–173]. With the invention of the laser source, emitting high intensity and high coherent light, the field of optical metrology has evolved leaps and bounds. Laser speckles which were earlier considered as noise now hold one of the most significant positions in the area of metrology [2,174,175].

The shape and size of laser speckles depend on the state of the incident wavefront. Thus, any modulation occurring to incident wavefront which may be due to a change in the refractive index will change the properties of the resulting speckles [50,176]. This relation between wavefront and speckle can be exploited by computing the spatial correlation coefficient by comparing the speckle pattern corresponding to different values of the measured quantity. We have already proposed techniques for measuring optical rotations induced due to the magneto-optic Effect [52] as well as due to the phenomenon of optical activity [54]. This technique is also applied for remote measurement and monitoring of temperature changes [53] and to estimate the out-of-plane displacement of the image plane [177]. Thus, this technique when amalgamated with a proper framework can be utilized to fabricate portable devices intended for the measurement of physical and optical properties of materials. Researchers have also recently demonstrated the use of speckle patterns for measuring the refractive index of glass which involves Fresnel transforms and speckle correlation [178].

The domain of 3D printing has undergone expeditious advancement in recent times that has changed the face of sensor fabrication. With this cutting-edge technology of 3D printing, a sensor's performance and its functionality can be immensely improved. 3D printers have enabled us to manufacture components with complex geometric shapes which has catalyzed its applications either for fabricating the whole sensor or some specific functional components [179]. Apart from the industrial and technical utility, 3D printers, for example, have found their applications in the field of microscopy as well, where the printed structure not only looks more elegant but also aids in the development of the microscope's functionality by providing a sturdy framework [180,181]. 3D printed version of a device can enhance the outcomes with an additional benefit of presentable form factor.

A simple compact and relatively inexpensive technique using laser speckles, which measures RI with high accuracy and has high sensitivity toward small change in refractive index values will be highly appreciated. The simplicity and compactness

of such a technique will allow it to be incorporated in a single mould and thus can be presented as a stand-alone portable device. Here an accurate technique that is employing speckle decorrelation for the measurement of the refractive index of transparent liquids is proposed. Moreover, due to the simplicity of the technique, a hand-held 3D printed refractometer is developed and demonstrated.

3.2.1 Theory behind refractive index measurement

In the presented technique, refractive index measurement is based on Snell's law and laser speckle correlation (Fig. 3.15). As light passes from air into a liquid medium it slows down [125–127]. Due to this phenomenon, the objects immersed in water appear to be shifted. Higher the concentration of the fluid, the slower the light travels through it, and more significant is the shift. It can be seen from Fig.(3.15) that when light from a point source is projected through the chamber containing a liquid solution, the curvature of the wavefront incident on the diffuser depends on the apparent position of the source. This apparent position, in turn, depends upon the refractive of the fluid kept inside the chamber. As the refractive index of the fluid changes, the apparent position of the point source changes, thereby changing the curvature of the incident wavefront. Since the intensity, shape, and position of the speckle pattern depend upon the wavefront impinging on the diffuser, any change in the refractive index of the fluid inside the chamber will change the speckle intensity distribution at the sensor plane. Moreover, the change in wavelength (due to change in refractive index) of the incident probe beam while passing through the medium also contributes to the change in the speckle pattern.

Thus, quantification of the change in the speckle pattern, due to apparent shift in the position of point source and the change in wavelength, can be utilized for measuring changes in the refractive index. Change in the speckle patterns is computed by comparing the speckle patterns recorded for solutions of different refractive indices (concentrations) with that recorded for a reference solution (distilled de-ionized water). The correlation coefficient and the change in correlation coefficient is computed using Eq. (2.8) and Eq. (2.9) respectively.

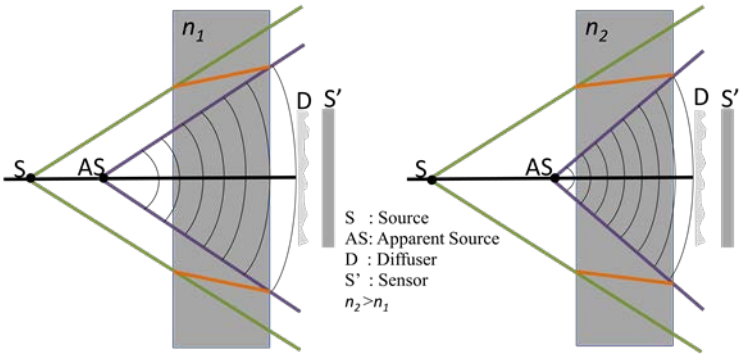

Fig 3. 15: Change in the curvature of the wavefront striking the diffuser, with a change in the refractive index of the fluid inside the test chamber. $n_2 > n_1$ *, where* n_2 *and* n_1 *are the refractive indices of the test fluids inside the chamber.*

For a given value of refractive index range, the sensitivity of the technique (minimum measurable refractive index change) can be improved by increasing the path length of the laser beam through the fluid.

3.2.2 Development of compact device for Refractive Index Measurement

Fig. 3.16 shows the schematic of the setup used for determining the change in the refractive index. The setup comprises a laser diode (power <5 mW, λ= 650 nm, random linear polarized), whose output is allowed to pass through a pinhole (30 μm diameter) generating a spherical beam. This beam then passes through the chamber (volume = 1 cm^3) made up of fused silica used to contain the liquid whose refractive index is to be measured. A ground glass diffuser (1 mm ×1 mm) is placed at the exit face of the chamber to generate the speckle pattern (objective speckle) which is recorded by a digital array (webcam sensor with 3.2 μm pixel pitch and 256 ×256 pixels exposed). During the construction of the device, the Nyquist sampling criterion is satisfied by placing the webcam 2 cm away from the ground glass diffuser so that the speckle size at the recording plane is at least twice the sensor pixel size.

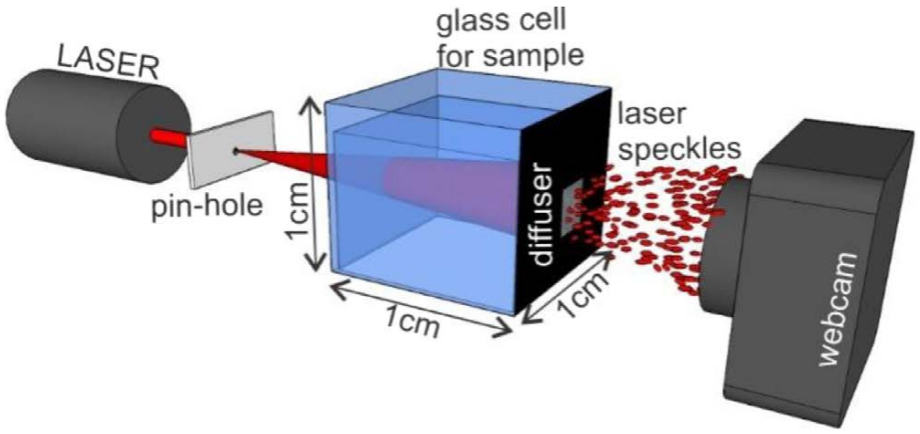

Fig 3. 16:Schematic of the technique used for the determination of change in refractive index

A 3D printer (Make3d.in, Prusa, 1.75 mm ABS filament) is employed to fabricate a frame of the device, based on the proposed technique, leading to a compact prototype of the stand-alone device to measure a small change in refractive index. The 3D printed hand-held refractometer is 7.5 cm long, 7 cm wide and has a height of 4 cm as shown in Fig. 3.17 a. Two batteries of 1.5 V are used to supply power to the laser diode as shown in Fig. 3.17 b. The laser diode, pinhole, the chamber containing the solution, webcam sensor and battery for supplying power to the laser diode are affixed at their respective positions inside the refractometer module as shown in Fig. 3.17 c. The idea behind using the 3D printer is to lay emphasis and attention to the small form factor achieved by the use of the presented technique. Although the optical components involved in the technique are not 3D printed, the 3D printed module serves the purpose.

Fig 3. 17: (a) The 3D printed refractometer (b) the power supply assembly that provides the necessary voltage and current to the laser diode. (c) Top view of the device showing all major significant components.

Furthermore, the webcam of the device can be accessed by a smart-phone through an OTG (On-The-Go) cable and images (speckle patterns) stored in its memory as shown in Fig. 3.18. These images can be transferred to a PC for further analysis.

Fig 3. 18: A speckle pattern recorded by the smartphone, when attached to the webcam of the refractometer with the help of a USB OTG

The developed device is tested for refractive index measurement by preparing sugar solutions corresponding to different concentrations and recording a series of speckle patterns (at the rate of 25 Hz for 30 s). During the analysis 30 speckle patterns out of all the recorded patterns are used. Once the speckle patterns are extracted, the correlation coefficient is determined by comparing the speckle patterns corresponding to the sucrose solution (test solution) with speckle patterns recorded using distilled, de-ionized water (reference solution) in the test chamber using the technique shown in Fig. 2.1. The time average of these values is used to calculate the change in correlation coefficient using Eq. (2.9). The use of the computed speckle decorrelation value in the calibration plot yields the refractive index of the test solution. Since a speckle pattern corresponding to a reference solution is always recorded before recording the speckle pattern corresponding to the test solution and since the chamber remains the same throughout the experiment, the effect of the chamber's material (which in our case is fused silica) on the measurement is nullified. Moreover, as the study deals with a very small change in the refractive index, the variation in reflectance of the source at the liquid chamber interface for different solutions can also be neglected.

3.2.3 Calibration and Measurements

For testing the system's ability to determine the refractive index of transparent liquids, simulations are carried out initially. For performing the simulations, all the experimental parameters such as chamber size, point source to the diffuser distance, a diffuser to sensor distance, sensor pixel size, etc. are considered the same as in the actual experimental setup. Angular spectrum propagation integral of scalar diffraction theory is used to simulate the propagation of the beam from the diffuser to the sensor plane [182]. Fig. 3.19 shows one of the simulated speckle patterns considering water (refractive index = 1.333) inside the test chamber.

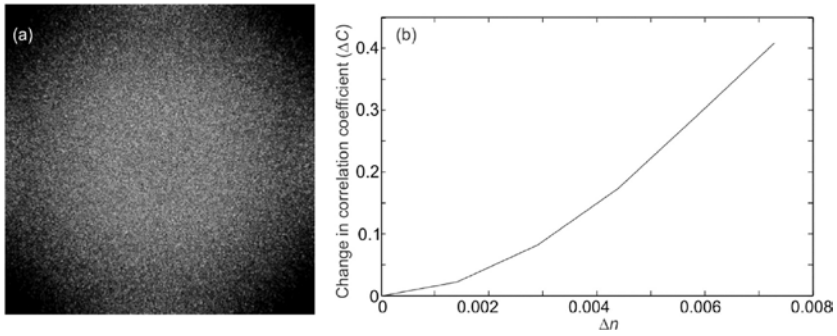

Fig 3. 19: (a) Simulated speckle pattern corresponding to water (n = 1.333). (b) Change in correlation coefficient with a change in refractive index in the case of simulated speckle patterns.

Six speckle patterns corresponding to equally spaced refractive indices in the range 1.333 to 1.3403 are generated. For each refractive index value, the speckle pattern generated for water is used as the reference pattern for calculating the change in the correlation coefficient. Fig. 3.19 b shows the computed change in the correlation coefficient as a function of change in the refractive index. From the simulations (Fig. 3.19) it can be seen that the proposed technique is able to discriminate between very small changes in the refractive index. It can also be concluded from the preliminary results obtained by simulations that the range of the technique is limited. However, the range of the system, in this case, relies on the sensitivity of the system which in turn depends on various factors such as wavelength, length of the chamber used to contain liquid, aperture size and distance of the sensor from the diffuser. The range of the system can be increased either by increasing the

distance of the sensor from the diffuser or by employing an aperture with a smaller size. This may create more diffraction, lead to loss of higher frequencies and increase the speckle size. The system with the increased speckle size will respond less to the change in measuring quantity thereby decreasing the sensitivity and increasing the range. Another way to vary the range is by iteratively changing the reference solution and comparing the test solution with the new reference. This can help in preventing the correlation values from collapsing for higher change in the refractive index. It may be noted that in this particular system it is not possible to measure the rotation of polarization due to the sugar solution.

Before applying the proposed system to measure refractive indices of unknown solutions, the system is calibrated using solutions of known refractive index ranging from 1.3344 to 1.3403 with the step of 0.0014. Sucrose solutions of different concentrations are prepared to have the required refractive index. Initially, distilled and de-ionized water, which acts as a reference solution, is filled inside the chamber and the corresponding speckle patterns were recorded. Thereafter the water is replaced with the sucrose (sugar) solution with known refractive index (after calibration, test solution was used to fill the chamber). The recorded speckle patterns corresponding to the known refractive index solutions are then compared with the reference speckle pattern generated by de-ionized distilled water (refractive index = 1.333) to quantify the change in refractive index. This is repeated for sucrose solutions of other known concentrations (refractive indices). Fig. 3.20 shows the recorded speckle patterns for the various refractive index of sucrose solutions used in the experiment.

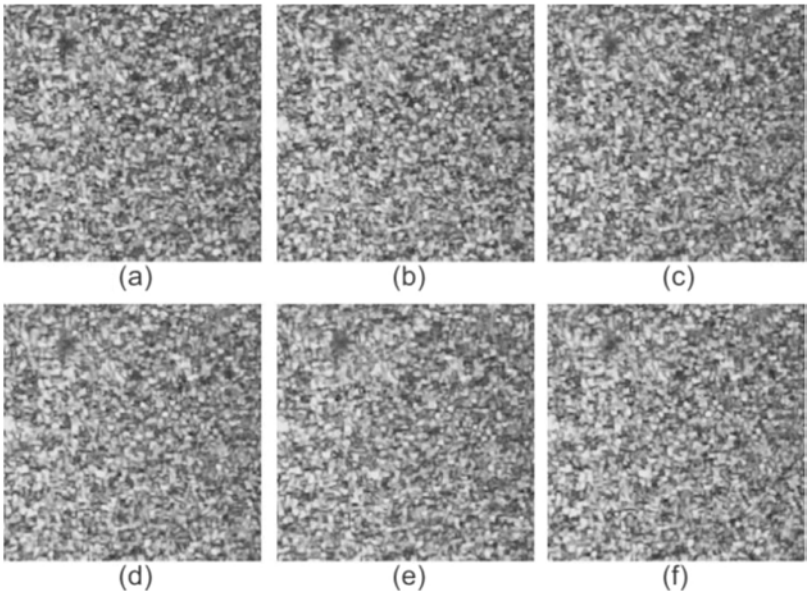

Fig 3. 20: Recorded speckle patterns for sugar solutions of different refractive indices. (a) Δn = 0 (distilled and de-ionized water) (b) Δn = 0.0014, (c) Δn = 0.0029, (d) Δn = 0.0044, (e) Δn = 0.0058 and (f) Δn = 0.0073.

During the analysis, correlation coefficient values are obtained by comparing 30 frames of the recorded speckle patterns corresponding to each concentration of sugar solution with 30 frames of the recorded speckle patterns with water inside the chamber. The measurements are repeated seven times for each concentration and the average correlation coefficient was obtained. Fig. 3.21 shows the average of the time variation of the correlation coefficient obtained from 7 measurements. Fig. 3.21(b) shows the change in the correlation coefficient as a function of the fluid concentration. It can be seen that the change in correlation coefficient varies non-linearly with the refractive index difference. This is due to the spherical nature of the wavefront impinging the diffuser. Here the correlation only depends upon the shape of the incident wavefront (spherical) and hence the change is also expected to be non-linear. Thus, the nonlinear behavior of change in correlation values (ΔC) obtained from the simulations is verified by the experimental data. Fig. 3.21(b) is also the calibration plot for the technique which is obtained from values of seven trials each for six different refractive index solutions including water.

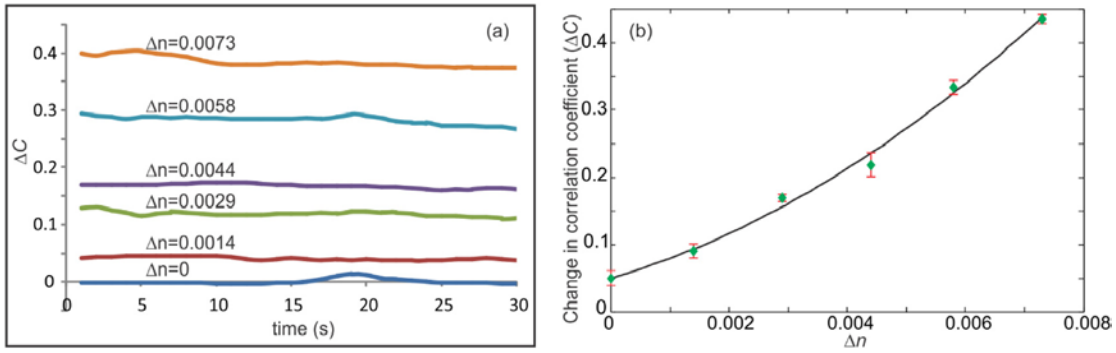

Fig 3. 21: (a) Time variation of the correlation coefficient after averaging over 7 measurements for each refractive index value. (b) Calibration curve: change in the speckle correlation coefficient (ΔC) with a change in refractive index.

It is observed in Fig 3.21 (a) that the change in correlation values for higher concentration decreases with time. This can be due to the fact that at higher concentrations, as time passes the turbulence in the solution arise due to multiple scattering, decreases, and thus the change in correlation coefficient may also decrease. The calibration values are fitted using second-degree polynomial (solid line in Fig. 3.21 b). Before measuring the unknown refractive indices, the resolution of the system is calculated. It is determined by averaging the standard deviation obtained for 7 data sets for each concentration during the calibration process and it turns out to be 0.00038. After calibrating the system, the calibration curve is used to determine the refractive indices of unknown solutions. Refractive indices (concentrations) which are in the range of the calibration plot but are different than the values used for calibrating the system, were prepared. Speckle patterns for these unknown refractive indices are recorded and the change in correlation coefficient was computed by comparing it to the reference (distilled & de-ionized water). From these values of change in the correlation coefficient (ΔC), the respective change in the refractive index is measured using the calibration curve. Table 3.1 shows the error in the measurement of the refractive index by comparing the change in the refractive index obtained by the proposed technique with the theoretical values. It can be seen that the system is able to measure small refractive index difference with an average error of less than 4.5%.

Table 3. 1: Measurement using the proposed technique and corresponding error

Change in refractive index (Δn)	(Δn) obtained using correlation value	% Error
0.00190	0.00180	4.83
0.00380	0.00352	7.45
0.00541	0.00535	1.16

3.3 Discussion and Future Scope

Although the measurement principle described in this chapter for the quantities is different, the aspects that are common in both measurements are the simplicity of the experimental arrangement, the compactness of the system and the accuracy of the technique. It is also demonstrated that the simplicity and compactness of the experimental arrangement assist in developing a handy, working prototype for refractive index measurement with the help of 3D printing technology.

The chapter demonstrates applications of the Speckle correlation technique wherein the experimental arrangements do not include any moving or mechanical part. As the system is very sensitive towards the state of the wavefront, any change in the wavefront due to the optical rotation and the change in the refractive index are directly reflected upon as a change in the speckle pattern. Thus, even a small change in the state of polarization and the refractive index results in an appreciable change in the resulting speckle pattern making the technique very responsive to polarization and refractive index change. By employing the speckle correlation technique, low optical rotation due to Faraday Effect and Optical activity were measured.

The cost of these experimental setups can vary depending upon the price of the two main components: Source and Sensor. The use of a laser pointer and a CMOS webcam can reduce the cost of the system gives comparable results comparable compared to the systems that use a gas laser and a CCD camera which are costly that can elevate the price of the system. Similarly, the sensitivity and the range of the systems can be customized. The distance of the sensor from the speckle producing surface is one of the parameters that can affect the sensitivity and range

of the system along with altering the length of the medium traversed by the beam and the size of aperture at the diffuser.

The study can be extended to the field of biomedical instrumentation where determining blood glucose level accurately is of great importance. This objective can be achieved in two steps, initially applying the proposed refractometer for concentration measurements and at a later stage using the already demonstrated technique of measuring sugar concentration which works on measuring the rotation caused by optical active materials. Since the second technique relies on the optical activity it can play an important role in decoupling the effects due to the concentration of salt and concentration of sugar in the blood plasma. Also quantifying the refractive index of various biological samples can be helpful in their characterization, identification, and discrimination. As the technique works by detecting the change in speckle pattern (generated by a ground glass diffuser) arising due to change in the incident wavefront, this technique may show inefficiency when dealing with thicker dynamic samples, which generates uncorrelated speckle patterns, using which the change in refractive index will be very difficult to trace. Presently the technique is being modified by the introduction of variable apertures at the diffuser to achieve variable detection ranges albeit with different sensitivity.